1-1-2008

The fundamentals of coke dissolution in the deadman area of the blast furnace

Michael Chapman
University of Wollongong, mchapman@uow.edu.au

Brian J. Monaghan
University of Wollongong, monaghan@uow.edu.au

Sharon A. Nightingale
University of Wollongong, sharon@uow.edu.au

John G. Mathieson
BlueScope Steel, John.Mathieson@bluescopesteel.com

Robert J. Nightingale
University of Wollongong, robertn@uow.edu.au

The Fundamentals of Coke Dissolution in the Deadman Area of the Blast Furnace

Michael W. Chapman[+], *Brian J. Monaghan*[+], *Sharon A. Nightingale*[+], *John G. Mathieson*[++] *and Robert J. Nightingale*[++]

[+] *Pyrometallurgical Research Group, University of Wollongong, Wollongong, NSW 2522, Australia*

[++] *BlueScope Steel Limited, P. O. Box 202, Port Kembla, NSW 2505, Australia*

Abstract

An experimental study characterising mineral layer formation at the coke-iron boundary during coke dissolution has been carried out. In this experimental study coke was added to the surface of an iron-carbon melt. Experiments were carried out at temperatures between 1450 and 1550°C for periods of time between 2 minutes and 120 minutes, before being quenched. Quenched samples were then sectioned and the solidified coke-melt interfacial region prepared for SEM and EDS analysis. SEM images and EDS analysis of the coke-iron interface revealed a mineral layer was present at the interface at all experimental temperatures and times. Further, it was determined that the layer was calcium aluminate based and that over time became progressively enriched with calcium. The predominant mineral layer was found to be composed of alumina, CA6, CA2 and CA phases, with the proportions of these phases dictating its morphology. At short experimental times the layer was predominantly alumina plus CA6 or CA6 plus CA2 with an open low density structure. At longer times the layer was predominantly CA2 plus CA with a dense structure. The change in morphology of the layer had a profound effect on the rate of the rate of carbon dissolution from the coke. The effect of this mineral layer on the rate of carbon dissolution has been interpreted as a change in the reaction control mechanism.

Introduction

The final carbon concentration of hot-metal leaving a blast furnace is thought to be established while the liquid iron percolates through the packed coke bed in the deadman and hearth areas of the furnace [1]. Consequently, the rate of carbon dissolution into liquid iron, and the factors contributing to the kinetics of the carbon dissolution in these areas, must be understood in order to allow the optimisation of the blast furnace. Blast furnace coke typically contains 8-12% by mass inorganic mineral matter [2], derived from the mineral matter of the parent coals [3,4]. As coke is dissolved in the liquid iron, there is potential for the insoluble components of this inorganic mineral matter to form a layer at the surface of the coke inhibiting carbon dissolution [5-12].

There is a significant body of research that has focused on the kinetics of coke dissolution into iron [6,10,11,13-18]. Coke dissolution into iron is generally considered to be controlled by first order kinetics and is frequently described by the rate of carbon dissolution if liquid side mass transfer limits the dissolution reaction, as presented in equations 1 and 2.

$$J = \frac{D}{\delta}\left([C]_{sat} - [C]_{bulk}\right) \qquad \text{or} \quad J = k_m\left([C]_{sat} - [C]_{bulk}\right) \tag{1}$$

Under the assumption of ideal mixing within the melt, the mass balance for carbon can be integrated (assuming A, V, and k_m are all time independent) as,

$$\frac{V}{A}\ln\left(\frac{[C]_{sat} - [C]_o}{[C]_{sat} - [C]_{bulk}}\right) = k_m t \tag{2}$$

where,

J = Flux (composition.m.s^{-1})

D = Diffusion Coefficient of carbon in liquid iron (m^2.s^{-1})

δ = Effective boundary layer thickness (m)

$[C]_{sat}$ = carbon concentration at carbon saturation

$[C]_{bulk}$ = Bulk carbon concentration in melt

$[C]_o$ = Initial carbon concentration of bulk at t=0

V = volume of melt (m^3)

A = area of reaction interface (m^2)

t = time (s)

k_m = mass transfer coefficient (m.s^{-1})

The generic term "ash" as used in the ironmaking literature can sometimes be misconstrued as the mineral matter residue from coke combustion, eg as determined in the proximate analysis, when in fact it may be a residual product of coke dissolution in iron. In this paper when discussing our results, the inorganic and mineral components of coke will be referred to as mineral matter. To ensure there is no misrepresentation of other researchers work, when referring to their work, the term ash will continue to be used.

Several researchers have reported on the role ash plays in reducing the rate of carbon dissolution into iron from coke [6,10,17]. Orsten and Oeters [10] reasoned that a solid ash product would be distributed across the reaction surface, reducing the available contact area between the carbonaceous material and the melt, however, if the ash product was liquid, it could be flushed away from the interface, reducing this effect. Gudenau et al [6] indicated that an ash film formed on the surface of the coke, and that presence of this film was significant in reducing the rate of carbon dissolution from the coke. This study also found that the addition of refractory oxides, CaO, MgO, Al_2O_3 to the coke further decreased the dissolution rate, while additions of iron oxide enhanced the dissolution rate.

Following experiments that used a sessile drop apparatus to react a drop of iron with a carbonaceous substrate, Wu et al [19], McCarthy et al [8,9] and Khanna et al [7], reported on the presence and composition of the ash product at the droplet / carbonaceous material interface. General observations of the droplet surface in these studies indicate that although silica was contained in the carbonaceous material, there was none present in the ash at the interface. The ash at the interface was initially Al_2O_3, however as the reaction time increased, the proportion of CaO increased, after which the Al_2O_3 was observed to disappear from the droplet-coke interface and was replaced by an iron calcium sulphide. Although these studies are instructive in identifying potential features of a mineral matter layer at the metal coke interface, the coke-metal mass ratios used are not typical of those found in the blast furnace. Under industrial condition the coke-metal ratio will be much lower, with the potential for silicon and sulphur levels of the metal as a result of coke dissolution to also be much lower. This would have a significant impact on any mineral layer formed at the interface [5]. Khanna et al [7] also observed a significant change in the rate of carbon dissolution over time in some chars. Chars with high CaO levels displayed a two stage behaviour, whereby after a period of time the rate of dissolution would decrease significantly. This two stage behaviour was attributed to the increased deposition of calcium based reaction products blocking the reaction surface.

In a recent study by the current authors [5,12], examination the coke-iron interface of coke samples immersed in liquid iron showed that the type of mineral layer formed was temperature dependant. No mineral layer was observed at 1550°C, while at lower temperatures (1500-1400°C) a mineral layer was observed. The formation of the layer was described in terms of a temperature activated time dependant sintering/fusion mechanism. In this study it was also found, consistent with the work of Wu et al [19], McCarthy et al [8,9] and Khanna et al [7], that SiO_2, although the largest single component of the mineral matter in the unreacted coke was essentially absent from the coke-iron mineral layer.

There has been no definitive study published in the literature that has characterised the development of the mineral matter layer with time and temperature and its affect on the coke (carbon) dissolution. Characterising the mineral layer's development is the focus of this study and the experimental results presented in this paper.

Experimental

A series of coke (carbon) dissolution experiments were performed whereby 10g of crushed coke (-2mm + 0.5mm) was added directly to the top surface of 164g of liquid iron 2 mass% carbon alloy. The melt plus coke were held at temperature for a period of time ranging from 2 to 120 minutes. At the end of this time, the crucible containing the melt and coke was quenched by lowering it into a water cooled stainless steel quenching chamber fitted to the bottom of the furnace. The experiment including the quenching was carried out in a dry argon atmosphere. The argon gas flow rate during the experiment was 0.94l/min and was increased to 9.4l/min during quenching. After quenching the samples were sectioned and prepared for electro-optical examination. Experiments were conducted over the temperature range of 1450-1550°C. The temperatures were chosen to replicate what might be expected in the lower zone deadman area of a blast furnace. A schematic of the furnace and sample configuration is given in Fig. 1.

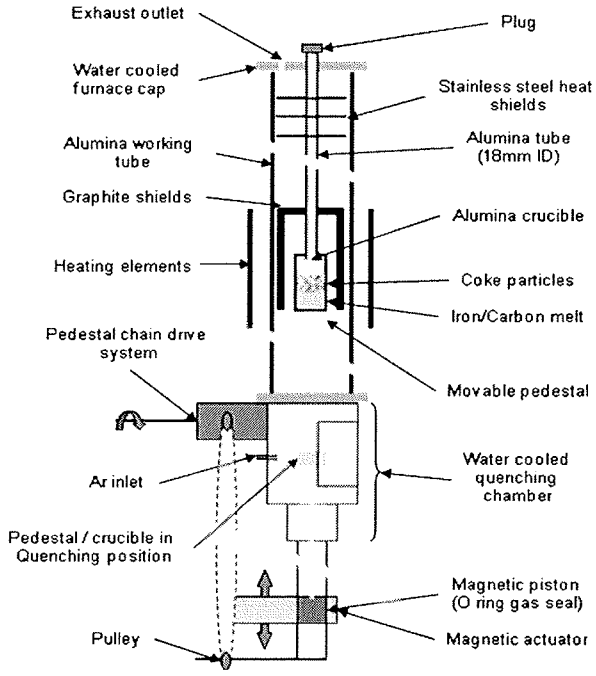

Fig. 1 A schematic of the furnace configuration used for the quenched series

A second series of coke (carbon) dissolution experiments were conducted whereby 35g of crushed coke (-2mm + 0.5mm) was added directly to the top surface of 572g of liquid iron carbon alloy. The melt was frequently sampled with a 1mm ID quartz tube over a period of 2 hours. The argon gas flow rate during the experiment was 0.72l/min. These experiments were conducted over

the same temperature range of 1450-1550°C as the quenched coke dissolution series. A schematic comparison of the samples used in both series of experiments is given in Fig. 2 and a comparison of the key geometric factors of both series is presented in Table 1.

Table 1 Key sample geometry of quenched carburiser cover series and carburiser cover series.

	Quenched coke dissolution experimental series	Coke dissolution experimental series
Crucible volume	$45cm^3$	$180cm^3$
Fe-C alloy mass	164g	572g
Coke mass	10g	35g
Interfacial area	$7.5x10^{-4}m^2$	$2.64x10^{-3}m^2$
Melt volume (Fe-2%C @ 1500°C)	$2.38x10^{-5}m^3$	$8.31^{-5}m^3$
Coke:Metal ratio	0.061	0.061
Melt : surface area ratio	$0.046g.cm^{-2}$	$0.046g.cm^{-2}$
Sample details	SEM – Horizontal Interface LECO C/S Machined from bulk	1mm pins drawn from melt

Raw Materials

The iron carbon alloy was prepared by melting appropriate amounts of electrolytic iron and coarsely crushed spectrographic grade graphite rod to achieve a 2% carbon-iron alloy prior to the addition of the coke. The coke samples used were provided by BlueScope Steel and contained approximately 0.4 – 0.45 mass% sulphur and 11.6 mass% inorganic material. The inorganic material can be considered to be refractory in nature. A detailed oxide composition measured by XRF after ashing at 815°C is given in Table 2. The lump coke was coarsely crushed to -20mm in a jaw crusher, then was further crushed in a roll crusher to obtain the desired -2mm + 0.5mm size fraction used.

Table 2: Composition of the of the oxide components in the coke in mass %.

SiO_2	Al_2O_3	Fe_2O_3	CaO	P_2O_5	MgO
54.8	32.3	4.9	2.9	1.42	1.0
K_2O	TiO_2	Na_2O	S	Mn_3O_4	
0.51	1.4	0.38	0.063	0.05	

Sample Preparation and Analysis

The quenched crucible containing the iron alloy and coke was impregnated with liquid resin under vacuum to preserve the coke-metal interface during sectioning. Lead shot was added to the top of the coke inside the crucible, before the resin impregnation to minimise coke movement during the vacuum impregnation procedure. The bottom section of the crucible was removed and iron samples for analysis were machined from the iron block. A vertical cut was made across the centre of the sample exposing the coke-metal interface. The interface was mounted and prepared for SEM analysis. Carbon and sulphur analysis was performed using a LECO CS-444 analyser. Analysis of other elements in the iron was performed by atomic emission spectroscopy, at the metallurgical laboratories of BlueScope Steel on disks of iron machined from the middle of the quenched iron sample.

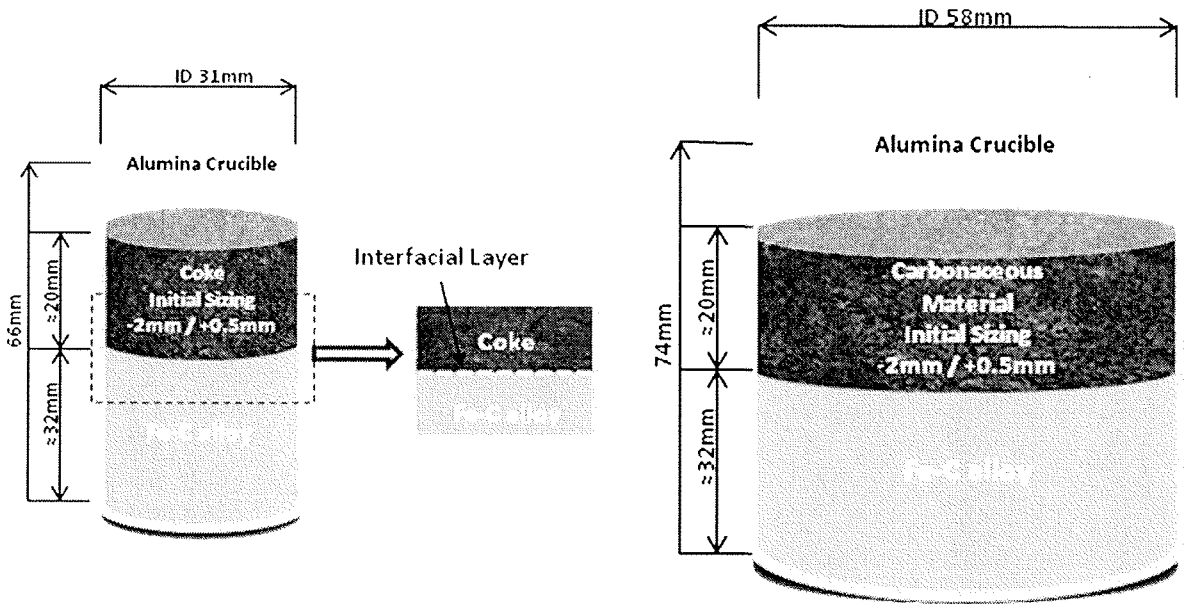

a) b)

Fig. 2 Schematic comparison between experimental samples used for a) Quenched coke dissolution series b) Coke dissolution series.

Results

Carbon transfer

Carbon pickup for the quenched and non quenched dissolution experiments, is plotted for 1450°C, 1500°C and 1550°C as a function of time in Fig.3. There is good agreement in the level of carbon pickup with time between the two experimental methods employed in this study. This agreement indicates that the same factors that affect the kinetics of carbon transfer from coke to the iron are active in both sets of experiments.

In the case of the 1450°C and 1500°C quenched carburiser cover results, the carbon level is seen to increase steadily before reaching a maximum of approximately 3.0 and 3.6 mass% at 60 and 40 minutes respectively. Beyond this there was little subsequent carbon pickup in the melt. In the case of the 1550°C quenched carburiser cover results, the carbon pickup was initially rapid, and although no clear plateau is observed the rate of carbon transfer to the melt slowed. This rate reduced over the experimental time with carbon reaching a maximum of approximately 4.67 mass% after 120 minutes of contact. The maximum carbon levels reached in these experiments are significantly below the carbon saturation levels calculated using MTDATA [20]. Melt compositions used to calculate the carbon saturation values are based on the average values beyond 60 minutes for 1450°C and 1500°C and beyond 90 minutes for 1550°C. These average melt compositions and the calculated carbon saturation values are given in Table 3.

Layer Formation

SEM analysis, involving electro-optical analysis, X-Ray mapping and EDS analysis was performed over large areas of the coke-iron interface. Typically, evidence of a mineral layer was observed in all samples at all experimental times from 2 minutes to 120 minutes over the 3 experimental temperatures of 1450°C, 1500°C and 1550°C. Due to the large numbers of samples

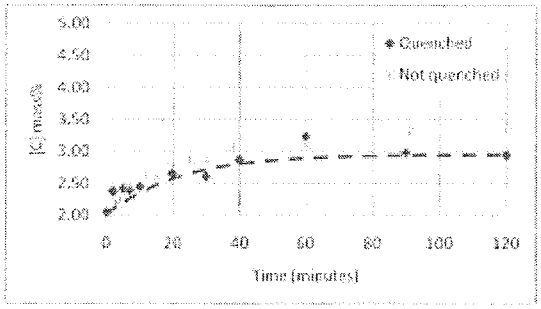

(a)

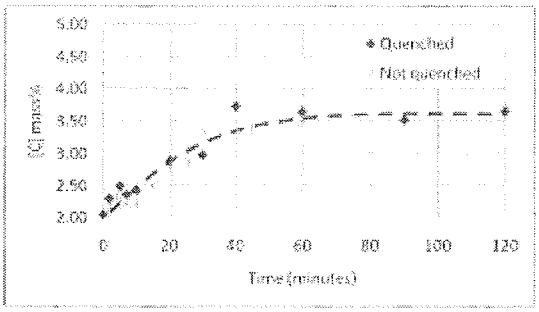

(b)

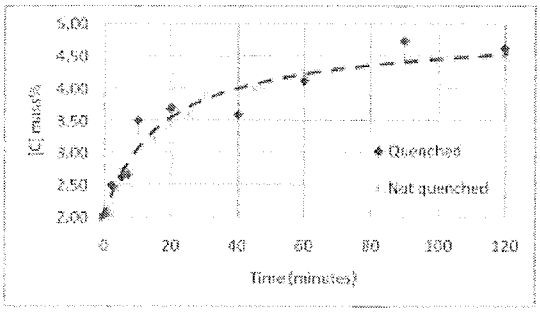

(c)

Fig. 3 [C] concentration versus time at (a) 1450°C (b)1500°C (c)1550°C

Table 3 Average melt composition beyond 60 minutes (1450°C and 1500°C) and beyond 90 minutes (1550°C) and calculated carbon saturation [20].

	$[C]_{avg}$	$[S]_{avg}$	$[Si]_{avg}$	$[Ti]_{avg}$	$[Mn]_{avg}$	$[C]_{sat}$
1450°C	3.05	0.008	0.063	0.033	0.03	5.09
1500°C	3.60	0.012	0.098	0.051	0.03	5.20
1550°C	4.67	0.013	0.130	0.050	0.03	5.32

and the large areas examined, only selected representative images are reported. The results reported below are observations and measurements of the coke-iron interface after quenching. Unless otherwise stated, it is assumed that the results reported and discussed are representative of the high temperature phenomena.

Upon cooling the iron-carbon alloys experience a significant increase in density, resulting in contraction of the melt surface away from the original iron-coke interface. This contraction of the melt results in either a gap between the melt and the original mineral layer, or the distortion of the original mineral layer as it adheres to the contracting iron surface. A typical section of interface is presented in Fig. 4. The mineral layer is observed following the profile of the iron surface, although the original liquid iron surface has contracted away from the mineral layer. The resulting voids are filled with resin during the metallographic preparation of the sample.

The composition of the mineral layer was found to be principally composed of calcium aluminates. The ratios of calcium and aluminium found in the mineral layer indicate that the mineral layer is composed of alumina, and the calcium aluminates, $CaO.6Al_2O_3$, $CaO.2Al_2O_3$ and

$CaO.Al_2O_3$. The melting points of these phases being 2053°C, 1830°C, 1762°C and 1602°C [21] respectively. The melting points of these phases are well above the experimental temperatures. There was no evidence of the quenched mineral layer being liquid at the experimental temperatures. Therefore it is assumed the original mineral layer was solid before quenching and the original solid structure and composition of the mineral layer is retained in the quenched sample.

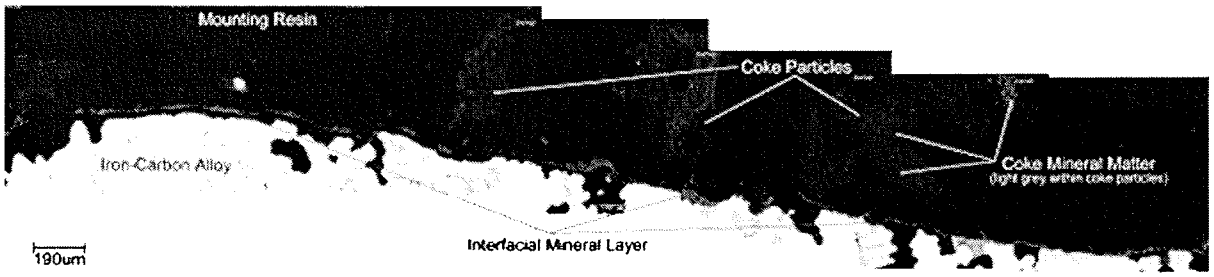

Fig. 4 QBSD SEM images of the quenched coke-mineral layer-iron interface, quenched after 5 minutes at 1500°C

The amount of material present in the mineral layer between the coke and liquid iron was observed to be increasing with reaction time. The morphology of this layer was also observed to change with time, transforming from an initial loose agglomeration of particles, through an acicular open structure before developing into dense layer. The level of calcium in the calcium aluminate was found to increase with both reaction time and temperature.

The initial stages of the formation of the mineral layer can be observed in Fig. 5 and Fig. 6. In Fig. 5 a partially dissolved coke particle is present near the melt interface. Although the iron has contracted away from the surface of the coke particle on cooling, the coke-iron interface is still evident. On the coke side of the interface, the original mineral matter (primarily made up of aluminosilicates) is contained in a carbon matrix. On the melt side of the interface, mineral matter that has been exposed as the carbon matrix dissolved and has accumulated at the melt surface. The accumulated material forms an agglomeration of loosely packed particles, primarily composed of Al_2O_3. Fig. 6, a higher resolution image of the Al_2O_3 layer shows the layer has an open pore structure.

Fig. 5 also illustrates the behaviour of silica at the coke-iron interface. Silica is regularly observed in undissolved coke particles present near the coke-iron interface however it is generally absent from the mineral layers that are formed at the coke-iron interface. This absence of SiO_2 from the mineral layer at the coke-iron interface is attributed to reduction of the SiO_2 by solute carbon in the melt. This has been discussed in detail previously [5].

Development of the mineral layer

Images representing the development of the coke-iron mineral layer are given in Fig. 7-10. As the coke dissolution reaction continues the predominant structure changes from a loose agglomeration of primarily alumina particles to an open porous network of acicular needles as shown in Fig. 7 and 8. These needles are still predominately Al_2O_3, but also contain an increased proportion of calcium, up to approximately 9 mass%. Further dissolution, increases the calcium enrichment of the mineral layer. This layer retains a relatively open structure however the fine needles evident in Fig. 7 and 8 are replaced by coarser structure shown in Fig. 9. The composition of the mineral layer has also continued to change with CaO comprising approximately 20 mass% of the layer. As the dissolution reaction time continues, further calcium enrichment of the mineral layer is observed, with CaO levels reaching in excess of 26 mass%. The structure of the

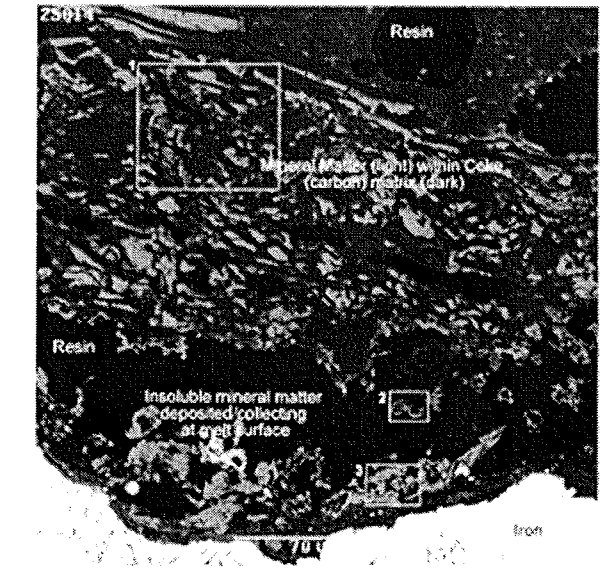

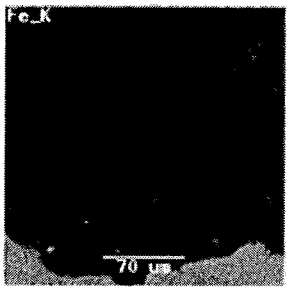

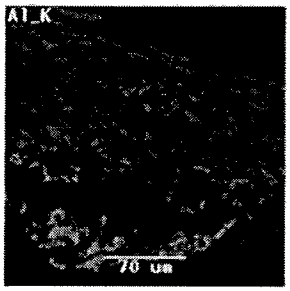

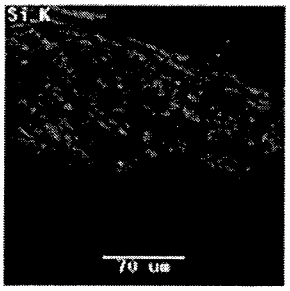

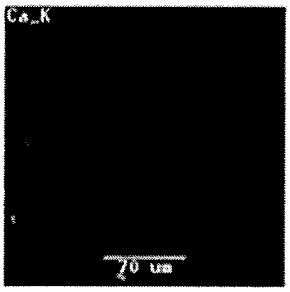

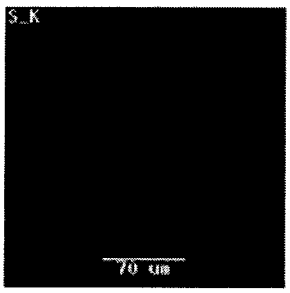

Fig. 5 QBSD SEM image and elemental x-ray maps of coke particle on the interface quenched after 2 minutes at 1500°C. Numbered regions have been analysed using EDS, the compositions given in Table 4.

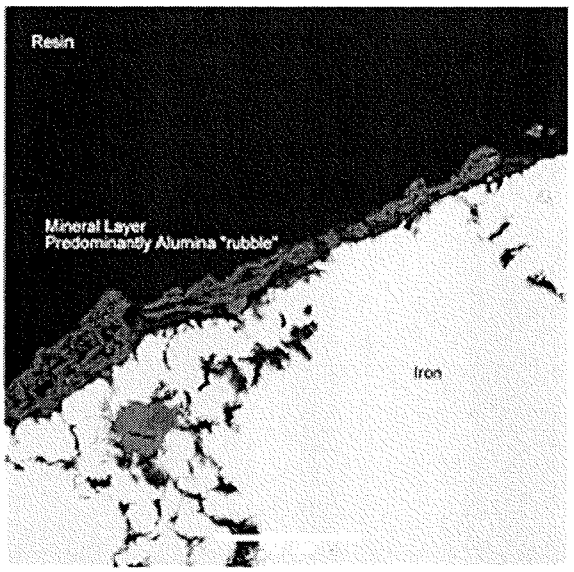

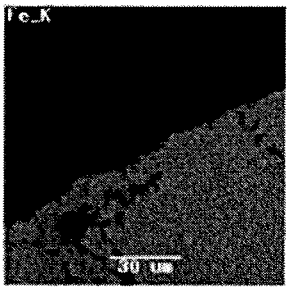

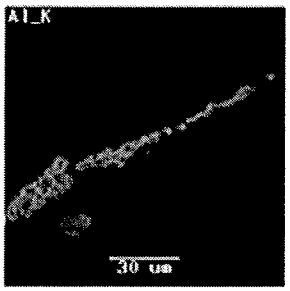

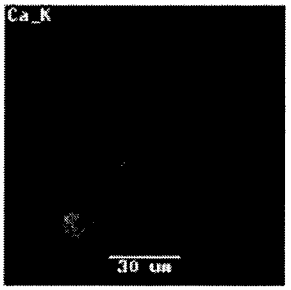

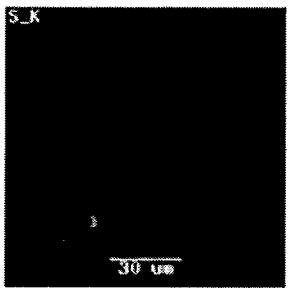

Fig. 6 QBSD SEM image and elemental x-ray maps of mineral layer quenched after 2 minutes at 1500°C.

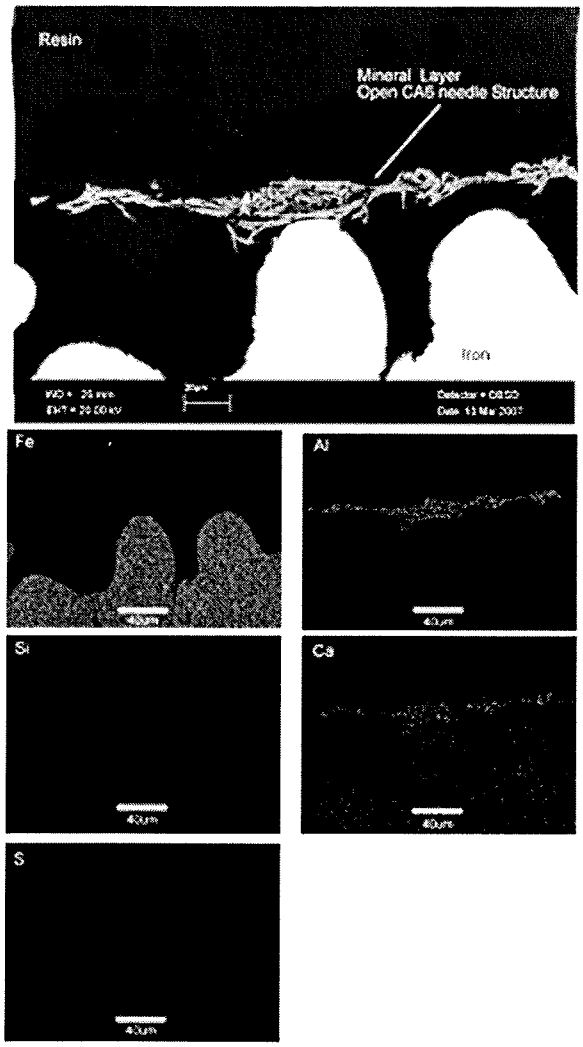

Fig. 7 QBSD SEM image and elemental x-ray maps of mineral layer quenched after 5 minutes at 1450°C. Numbered regions have been analysed using EDS, the compositions given in Table 4.

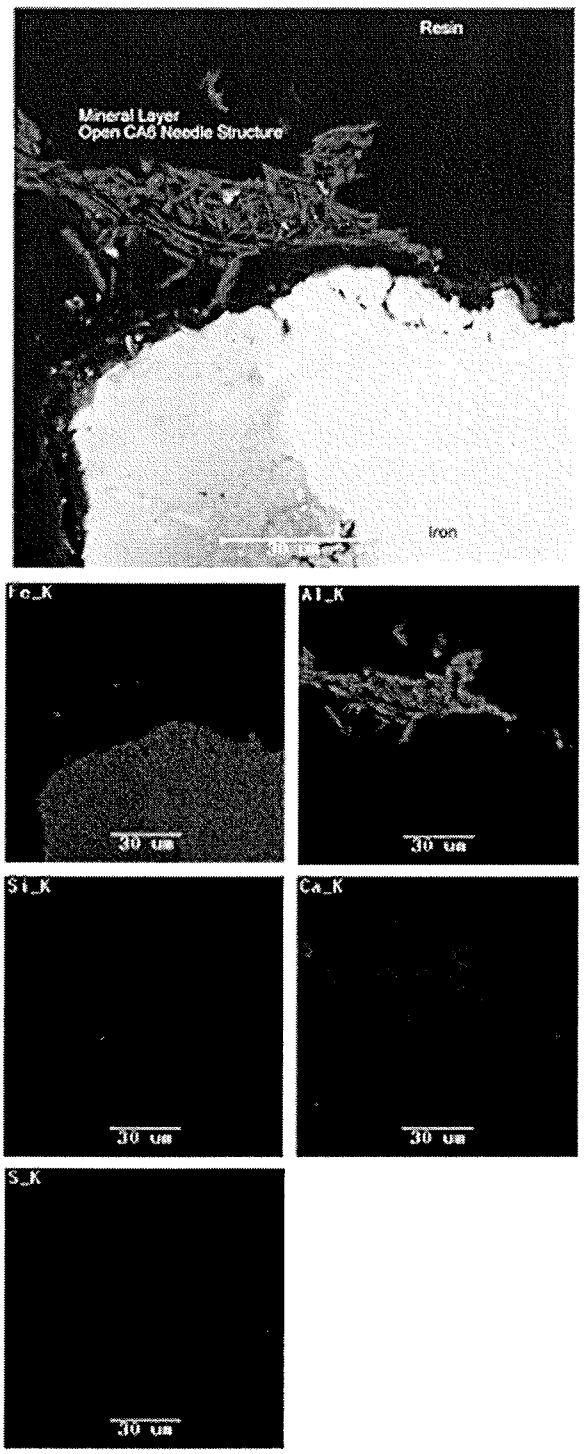

Fig. 8 QBSD SEM image and elemental x-ray maps of mineral layer quenched after 2 minutes at 1500°C.

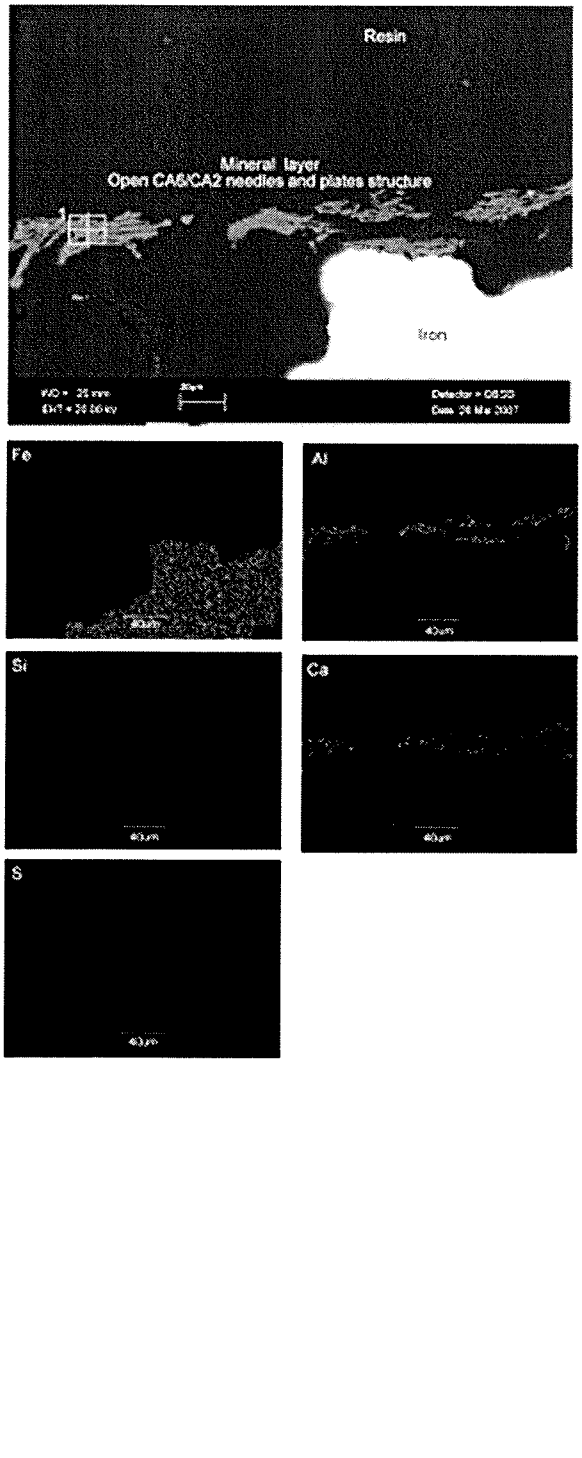

Fig. 9 QBSD SEM image and elemental x-ray maps of mineral layer quenched after 60 minutes ate 1450°C. Numbered regions have been analysed using EDS, the compositions given in Table 4.

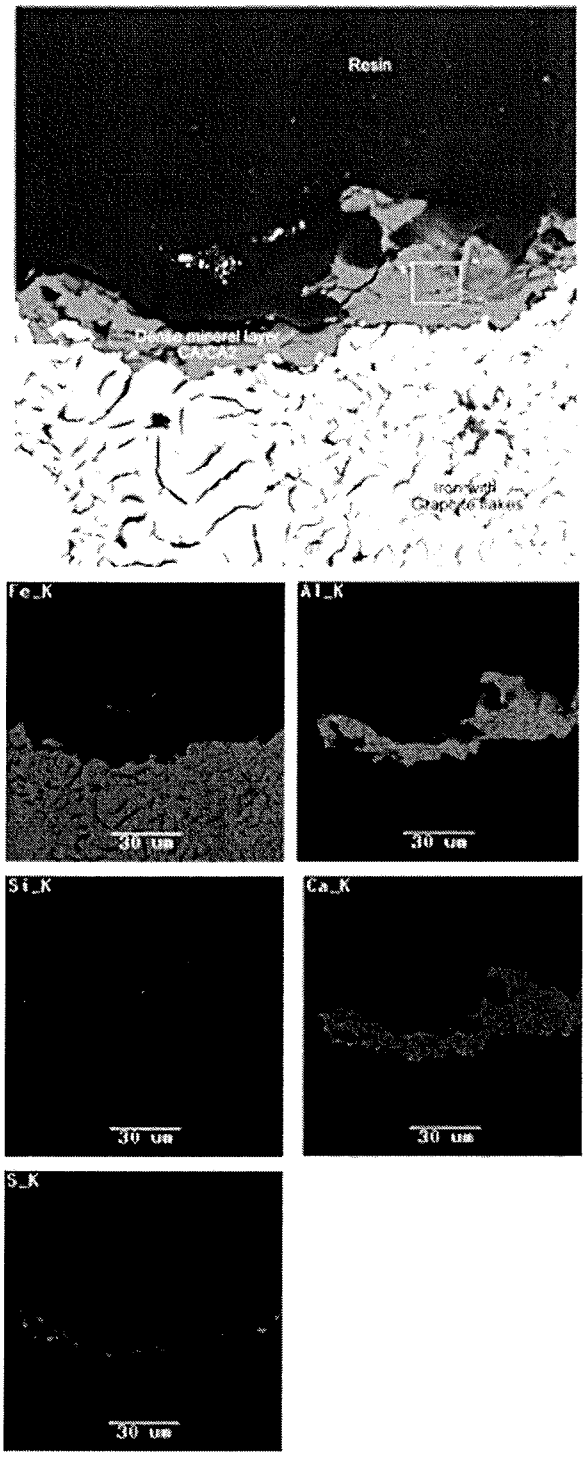

Fig. 10 QBSD SEM image and elemental x-ray maps of mineral layer quenched after 60 minutes at 1500°C. Numbered regions have been analysed using EDS, the compositions given in Table 4.

predominant mineral layer changes from being an open structure evident in Fig. 6 to 9, to a dense layer that is well bonded to the iron surface as shown in Fig. 10.

EDS analysis for regions indicated by numbered rectangles in Fig. 5 to 10 are given in Table 4. Molar ratios of CaO to Al_2O_3 are given for analysis regions of the coke-iron interfacial mineral layer. Where sulphur was present, it has been attributed to the CaS phase and the amount of CaO reduced accordingly. The role of calcium enrichment in the mineral layer at the melt interface can be understood by considering the CaO-Al_2O_3 binary phase equilibrium diagram (Fig. 11) [21]. There are three distinct calcium aluminates at the alumina rich end of the phase diagram. The structures of these calcium aluminates have been well characterised as they are important with respect to cleanness in the steelmaking process [22]. Key details of these calcium aluminates are given in Table 5. It should be noted that the authors are not suggesting that the calcium aluminates formed during coke dissolution have any role to play in cleanness issues later in the steelmaking process.

Table 4 EDS Analysis of Selected Regions of the Coke-Mineral Layer-Iron Interface.

	Fig. 5	Fig. 5	Fig. 5	Fig. 7	Fig. 9	Fig. 9	Fig. 10
Region	1	2	3	1	1	2	1
Al_2O_3	49.6	94	87.6	87.8	79.6	78.7	72.8
CaO	1.3	4.2	11.6	9.2	18.9	19.9	26.3
SiO_2	45.6	0	0	0	0	0	0.4
CaS	2.8	0	0	0	0	0	0
TiO_2	0.2	1.6	0.5	2.2	0	1	0
Other	0.5	0.2	0.3	0.8	1.5	0.4	0.5
Molar CaO/Al_2O_3		0.08	0.25	0.19	0.44	0.46	0.67

Table 5 Structure of the Alumina-Rich Calcium Aluminates

Phase	Abbreviation	Molar CaO/Al_2O_3 ratio	Typical Structure [22]	Melting Point [21]
$CaO.6Al_2O_3$	CA6	0.16	Acicular needles	1830°C
$CaO.2Al_2O_3$	CA2	0.5	Plate like crystals / Needles	1762°C
$CaO.Al_2O_3$	CA	1.0	Dense fine grains	1602°C

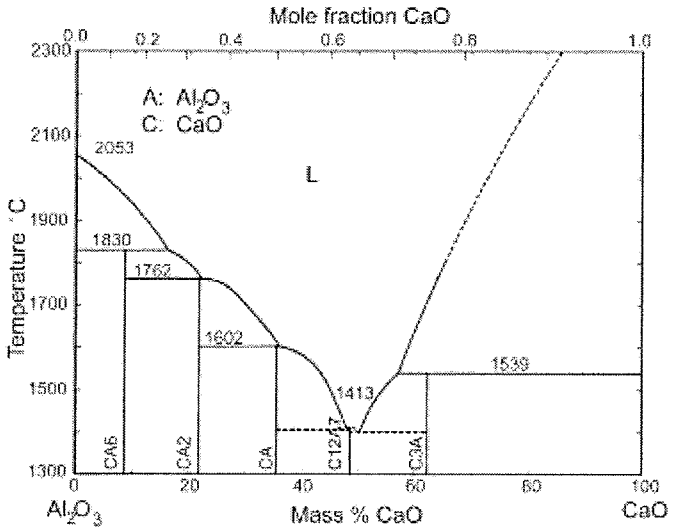

Fig. 11 CaO-Al_2O_3 phase diagram reproduced from Slag Atlas [21]

The calcium aluminate structures described in Table 5 are evident in the micrographs of the mineral layer presented in Fig. 6 to 10. EDS analysis of the needle like structures in Fig. 7 and 8 show that the molar CaO/Al_2O_3 ratio is 0.19, indicating that the mineral layer is predominantly the calcium aluminate CA6. The needle like acicular structure shown in Fig. 7 and 8 is typical of CA6. EDS analysis in the regions indicated in Fig. 9, shows a molar CaO/Al_2O_3 ratio of between 0.44 and 0.46. Such a ratio indicates a mixture of the calcium aluminates CA2 and CA6, with the mixture consisting of approximately 85% of the CA2 phase (as determined from Fig. 11). Such a structure could be expected to retain some of the fine acicular CA6 needles, but would also contain significant amounts of the larger, 2 dimensional plates of CA2 crystals. This is consistent with what is observed in Fig. 9. The dense calcium aluminate structure shown in Fig. 10, has a molar CaO/Al_2O_3 ratio of 0.67. This ratio indicates that the mineral matter layer contains approximately 66% of the CA2 phase with the remaining 34% being the CA phase (as determined from Fig. 11). The CA phase is a dense fine grained phase, and has developed around the CA2 phase, resulting in densification of the mineral matter layer.

Fig. 12(a) details the development of the coke-iron mineral layer in terms of its molar CaO-Al_2O_3 ratio. From Fig. 12(a) it can be seen as the calcium level in the mineral layer approaches a plateau. The time to reach this plateau decreases with increasing temperature. Also the level of calcium present in the mineral layer at the plateau increases with increasing temperature. Combining the information presented in Fig. 12(a) with the CaO-Al_2O_3 phase diagram (Fig. 11) the predominant calcium aluminate phases present in the coke-iron interfacial mineral layer can be determined and is shown in Fig. 12(b).

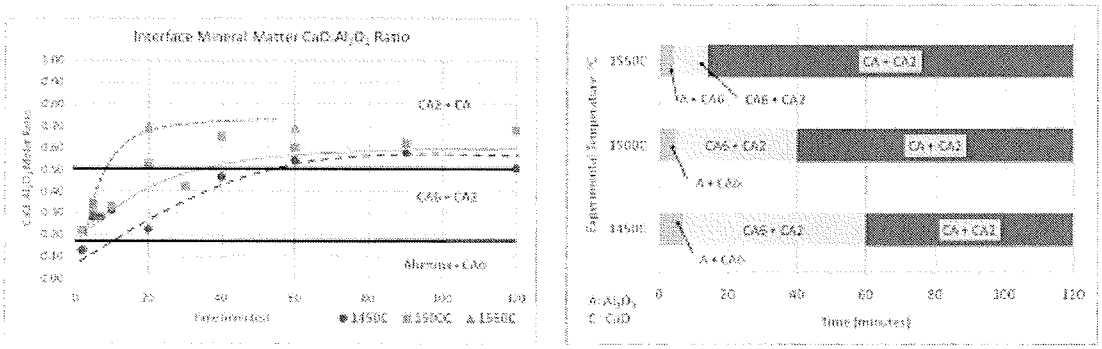

(a) (b)

Fig. 12 a) The molar CaO/Al_2O_3 ratio and b) the predominant phase at the melt interface versus experimental time.

Coke dissolution Kinetics

Coke dissolution into iron is generally considered to be a first order kinetic process and is generally described as being limited by liquid phase mass transfer of carbon in iron. The mass transfer coefficient, k_m, as defined in equation 2 for such a process can be evaluated from the slope of a plot of $\frac{V}{A}\ln\left(\frac{[C]_{sat}-[C]_o}{[C]_{sat}-[C]_{bulk}}\right)$ vs time. Such plots are given in Fig.13. The volume of the melt was taken to be $2.38\text{x}10^{-5}\text{m}^3$ (based on an assumed density of 6885kg/m^3 corresponding to a Fe-C 2mass% alloy at 1500°C [23]) and the area term was assumed to be the cross sectional area of the crucible.

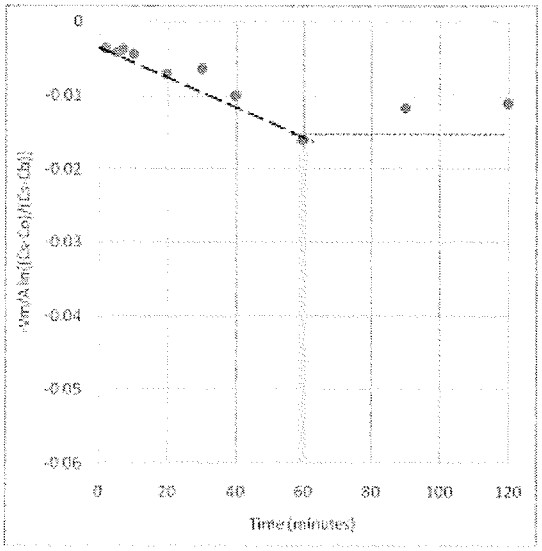

(a)

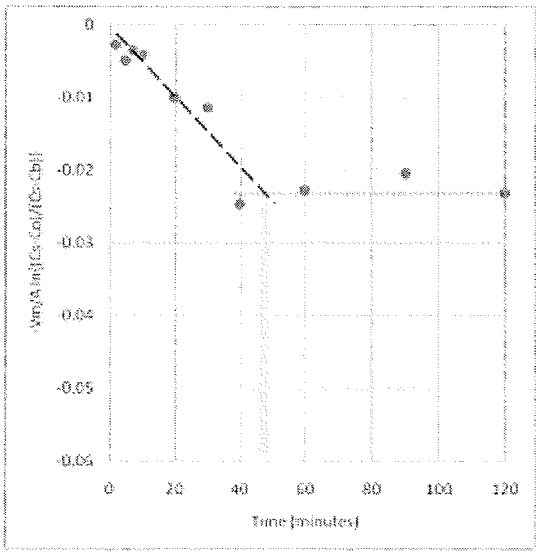

(b)

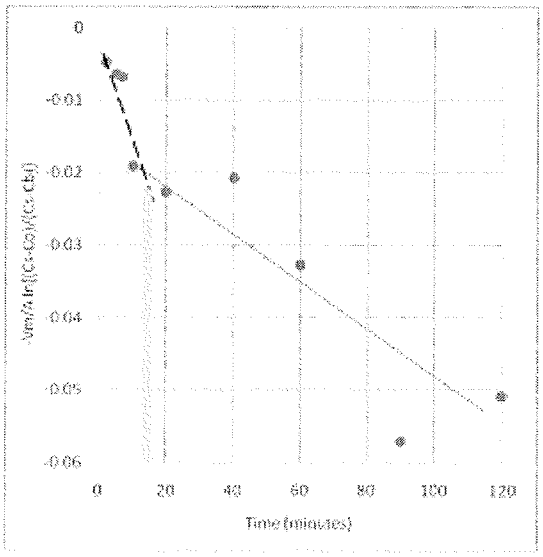

(c)

Fig. 13 First order mass transfer control plots (a) 1450°C (b) 1500°C (c) 1550°C

In Fig. 13, it can be seen that there is a significant change in k_m, the rate constant, after a period of time for all three temperatures. The change in k_m, a decrease in the slope, represents a slowing of the rate of coke (carbon) dissolution into the iron. Although presented here as first order mass transfer plots, the data has also been analysed as first order chemical control and second order kinetics. The change in slope with respect to the rate constants was also evident in these approaches.

Effects of structure on Kinetics

The change in the rate constant is coincident with the change in the predominant phases present in the mineral layer at the coke-iron interface from CA2/CA6 to CA/CA2. Accompanying this change in phase, there is a change in the morphology of the mineral layer from an open acicular structure to a more densely packed structure. This change in the morphology reduces the contact between the carbon in the coke and the liquid iron, and therefore slows the rate of coke (carbon) dissolution.

In the analysis a constant area term has been used for the contact between the coke and metal. This is a traditional approach in kinetic analysis. In reality, in the experiments there are two

distinct coke-iron contact regimes that may be characterised by two different area terms (or a continuous change in area from a relatively high value to a relatively low value). In constraining the area term to one value two mass transfer coefficients (k_m) have been obtained. It is likely that if the contact areas could be determined, the two k_m terms would reduce to a single value representing the overall rate of reaction. However, it is not possible to evaluate the contact area accurately in these types of experiments.

Other workers have inferred that the nature of the mineral layer that could form at the coke-iron interface will affect the kinetics of the carbon dissolution reaction [6-9, 17,19]. The results of this investigation demonstrate for the first time that the composition and subsequent morphology of the mineral layer formed affects the carbon dissolution reaction.

In the absence of a mineral (product) layer carbon dissolution into iron is considered to be a first order liquid phase mass transfer process [6,10,11,13-18]. In stating that the nature of the mineral layer formed during the coke dissolution affects the kinetics of the carbon dissolution reaction, a change in the reaction control mechanism is implied. On the assumption that mass transfer of carbon in the liquid iron is still in part rate controlling, the formation of the mineral (product) layer provides an additional controlling mechanism. This represents a change from simple mass transfer control to a mixed control regime where both mass transfer and the mineral (product) layer are active. Further, the changing nature of the mineral layer from and open (CA6/CA2) to dense (CA2/CA) structure could also be interpreted as a change in the reaction control mechanism.

Calcium Enrichment of the mineral matter layer

Calcium enrichment of the mineral matter at the melt interface is a key component of the formation of the mineral layer and its subsequent densification. Calcium enrichment levels are well above what should be expected solely from coke dissolution. Calcium levels in the iron melt have been measured throughout the experiment and were found to have changed from 24 ±1 ppm calcium initially to 22 ±1 ppm calcium after 120 minutes. A 10% increase in the molar CaO/Al2O3 ratio of the mineral layer would be achieved by a loss of 2.6ppm calcium from the iron. Therefore although the change in the experimental calcium level is significant, it does not fully explain the calcium enrichment of the mineral layer observed which is in the order of 200% for the CA6 to CA2 transition. Other workers have reported calcium mobility within coke [4,25] while calcium enrichment at the melt interface has been has been reported by other researchers[5,7,8,19]. This offers the possibility that enrichment of the mineral layer is also a result of calcium mobility within the coke. From the results reported it is not possible to distinguish between calcium in the mineral layer originating from the coke and the calcium from originating from the iron melt..

Application to the blast furnace

Though a mineral layer at the coke-iron interface could be expected to form as coke dissolves into liquid iron, it is whether it persists and develops at the interface that is important. If the mineral layer comes into contact with blast furnace slag it is likely the layer will be dissolved by the slag. If the mineral layer is formed in the absence of a slag phase, as would be the case in the blast furnace hearth, beneath the slag level, the mineral layer would persist and develop. This persistent mineral layer would significantly inhibit carbon dissolution from coke. It has been reported by Nightingale et a [26] that hot metal tapped from the blast furnace is not always at carbon saturation. This is unexpected as the coke and iron are in intimate contact in the hearth of a blast furnace for a significant period of time. The slowing of the dissolution rate observed in this work may provide an explanation for the findings why a blast furnace iron does not always reach carbon saturation.

Conclusions

A series of experiments has been carried out in an attempt to describe and characterise the mineral layer formed at the coke-metal interface as the coke dissolved into the liquid iron. It was found that

- The kinetics of carbon dissolution from the coke to the liquid iron were dependant on the structure of the interfacial mineral layer.
- The changing morphology of the mineral layer was directly related to compositional changes, with calcium enrichment of the mineral layer dictating the predominant phase and thus morphology of the mineral layer.
- The formation of the mineral (product) layer was interpreted as an additional rate controlling mechanism for the coke (carbon) dissolution reaction. This represents a change from simple mass transfer control to a mixed control regime where both mass transfer and the mineral (product) layer are active.

Acknowledgments

The authors would like to thank BlueScope Steel Ltd. and the Australian Research Council for supporting this research. They would also like to thank Dr Huijin Li, Senior Reseach Scientist, Australian Nuclear Science and Technology Organisation (ANSTO), for access to and assistance using ANSTO's SEM facilities.

References

1. Omori, Y.E. (ed), Blast Furnace Phenomena and Modelling, Elsevier Applied Science, London,(1987), p.58.
2. Loison. P, Foch. P, Boyer. A: Coke Quality and Production, Butterworths, London, UK,(1989), p.159.
3. Croft V: In Situ Reduction of Blast Furnace Coke Ash Ironmaking and Steelmaking,(1980), p. 116
4. Gornostayev S, Kerkkonen O, Harkki J: Occurrence and Composition of Some Mineral Phases in Tuyere Coke ISIJ International (Japan).45(2005), p. 1.
5. Chapman MW, Monaghan BJ, Nightingale SA, Nightingale RJ, Mathieson JG: Observations of the Mineral Matter Material Present at the Coke / Iron Interface During Coke Dissolution into Iron ISIJ International,(2007), p. 973.
6. Gudenau HW, Mulanza JP, Sharma DGR: Carburization of Hot Metal by Industrial and Special Cokes Steel Research 61(1990), p. 97.
7. Khanna R, McCarthy F, Sun H, Simento N, Sahajwalla V: Dissolution of Carbon from Coal-Chars into Liquid Iron at 1550 Dgc Metallurgical and Materials Transactions B,36B(2005), p. 719.
8. McCarthy F, Khanna R, Sahajwalla V, Simento N: Interfacial Phenomena Occurring During Iron/Char Interactions in a Blast Furnace ISIJ International,45(2005), p. 1261.
9. McCarthy F, Sahajwalla V, Hart J, Saha-Chaudhury N: Influence of Ash on Interfacial Reactions between Coke and Liquid Iron Metallurgical and Materials Transactions B,34B(2003), p. 573.
10. Orsten S, Oeters F: Process Technology Proceedings, Iron and Steel Society, Washington, D.C, USA, (1986),p. 143.
11. Wu C, Wiblen R, Sahajwalla V: 2000 Belton Symposium, Sydney, Australia, (2000),p. 409.
12. Chapman MW, Monaghan BJ, Nightingale SA, Nightingale RJ, Mathieson JG: Australia - China - Japan Symposium on Iron and Steelmaking, Liaoning science and Technology Publishing House, China, (2006),p. 90.
13. Cham ST, Sahajwalla V, Sakurovs R, Sun H, Dubikova M: Factors Influencing Carbon Dissolution from Cokes into Liquid Iron ISIJ International,44(2004), p. 1835.

14. Cham ST, Sakurovs R, Sun H, Sahajwalla V: Influence of Temperature on Carbon Dissolution of Cokes in Molten Iron ISIJ International,46(2006), p. 652.
15. Ericsson SO, Mellberg PO: Influence of Sulfur on the Rate of Carbon Dissolution in Liquid Iron Scandinavian Journal of Metallurgy,10(1981), p. 15.
16. Jones NW: Kinetics of Carbon Dissolution in Fe-C Alloy at 1550c Ironmaking and Steelmaking,25(1998), p. 460.
17. Mourao MB, Murthy GGK, Elliott JF: Experimental Investigations of Dissolution Rates of Carbonaceous Materials in Liquid Iron--Carbon Melts Metallurgical Transactions B,24B(1993), p. 629.
18. Orsten S, Oeters F: W.O. Philbrook Memorial Symposium Proceedings; , Iron and Steel Society, Toronto, Ontario, Canada, (1988),p. 27.
19. Wu C, Wiblen R, Sahajwalla V: Influence of Ash on Mass Transfer and Interfacial Reaction between Natural Graphite and Liquid Iron Metallurgical and Materials Transactions,31B(2000), p. 1099.
20. Davies RH, Dinsdale AT, Gisby JA, Hodson SM, Ball RGJ: Conference On Applications Thermodynamics on the Synthesis and Processing of Materials, ASM/TMS, Rosemont, IL, USA, (1994),p. p371.
21. Kowalski M, Spencer PJ, Neuschutz D. Phase Diagrams. In: (VDEh) VDE, editor. Slag Atlas. Dusseldorf: Verlag Stahleisen GmbH, 1995. p.39.
22. Kiessling R, Lange N: Non Metallic Inclusions in Steel,Vol. 2, The Metals Society, London,(1978), p.36.
23. Markert J, Potschke: Bestimmung Der Grenzflachenspannung Zwischen Graphit Und Kohlenstoffgesattigter Eisenschmelze Aus Dem Auftrieb" Arch Eisenhuttenw,50(1979), p. 53.
24. Oeters F: Metallurgy of Steelmaking, Verlag Stahleisen mbH, Dusseldorf, Germany,(1994), p.99.
25. Kerkkonen O, Mattila E, Heiniemi R: 55th Ironmaking conference proceedings, Iron & Steel Society Ironmaking Division, Pittsburgh, Pennsylvania, USA, (1996),p. 275.
26. Nightingale RJ, Dippenaar RJ, Lu WK: Developments in Blast Furnace Process Control at Port Kembla Based on Process Fundamentals Metallurgical and Materials Transactions B 31B(2000), p. 993.